A Comprehensive, Practical and Reliable Soft Start-Up and Shut-down Schemes for a Multi-Function Integrated EV Charger

2023 IEEE Energy Conversion Congress and Exposition (ECCE) | 979-8-3503-1644-5/23/$31.00 ©2023 IEEE | DOI: 10.1109/ECCE53617.2023.10362684

Ziwei Liang
Department of Electrical Engineering and Computer Science
University of Tennessee
Knoxville, TN, USA
zliang7@vols.utk.edu

Liyan Zhu
Department of Electrical Engineering and Computer Science
University of Tennessee
Knoxville, TN, USA
liyanz@vt.edu

Yue Sun
Department of Electrical Engineering and Computer Science
University of Tennessee
Knoxville, TN, USA
ysun79@vols.utk.edu

Jie Li
Department of Electrical Engineering and Computer Science
University of Tennessee
Knoxville, TN, USA
jli94utk@gmail.com

Ruiyang qin
Department of Electrical Engineering and Computer Science
University of Tennessee
Knoxville, TN, USA
ruiyangq@gmail.com

Arka Basu
Department of Electrical Engineering and Computer Science
University of Tennessee
Knoxville, TN, USA
abasu1@vols.utk.edu

Xin Xia
Department of Electrical Engineering and Computer Science
University of Tennessee
Knoxville, TN, USA
xxia6@vols.utk.edu

Rajib Bijukchhe
Department of Electrical Engineering and Computer Science
University of Tennessee
Knoxville, TN, USA
rbijukch@vols.utk.edu

Daniel Costinett
Department of Electrical Engineering and Computer Science
University of Tennessee
Knoxville, TN, USA
dcostine@utk.edu

Hua Bai
Department of Electrical Engineering and Computer Science
University of Tennessee
Knoxville, TN, USA
hbai2@utk.edu

***Abstract*—To build an integrated battery charger with multiple functions for electric vehicles (EVs), the system normally has several stages, such as AC/DC power factor conversion (PFC) converter, isolated and/or non-isolated DC/DC converters. Therefore, it is important to implement the start-up and shut-down procedure by coordinating multi-stage converters to avoid potential large inrush current or over voltage. This paper firstly proposed a highly integrated multi-stage battery charger for electric vehicles that offers multiple functions, including on-board charger (OBC), vehicle-to-load (V2L), wireless power transfer (WPT), all using a 400V battery, and auxiliary power module (APM) for a 12V battery. The control methods for each function are introduced. Based on the system configuration and characteristics of different functions, comprehensive system-level start-up and shut-down schemes are proposed for practical operation scenarios of OBC, WPT and V2L. Finally, a 400VAC/800VDC/22kW prototype is built and the effectiveness of the proposed start-up and shut-down schemes is verified by experiments.**

Keywords*—Integrated EV charger, multi-stage converter, soft start-up procedure, soft shut-down procedure

I. INTRODUCTION

Nowadays battery electric vehicles (BEVs) usually are equipped with 400V/800V high-voltage (HV) batteries and 12V low-voltage (LV) batteries, which supplies power to powertrain and other auxiliary loads onboard, respectively. Two types of charging methods, which are conductive such as OBC and wireless charging referred as WPT, can be used to charge the HV battery from the AC grid. APM is used to charge the LV battery from the HV battery [1].

Previously, different charging functions are achieved by separated units. Recent development of the EV chargers witnessed that system integration has become one of the main strategies to achieve lower cost and higher power density. By sharing some circuit among different converters, many different integration methods of OBC and APM have been introduced [2]–[4]. Compared with using separate transformers in [2], reference [3], [4] utilize a three-winding transformer to achieve compact design and less component count. Besides the conductive charging, WPT also has been widely explored because of the benefits of the convenience, safety, and automation [5]. Similar with the integration of OBC and APM, OBC and WPT can also be integrated [6], [7]. In [6], the

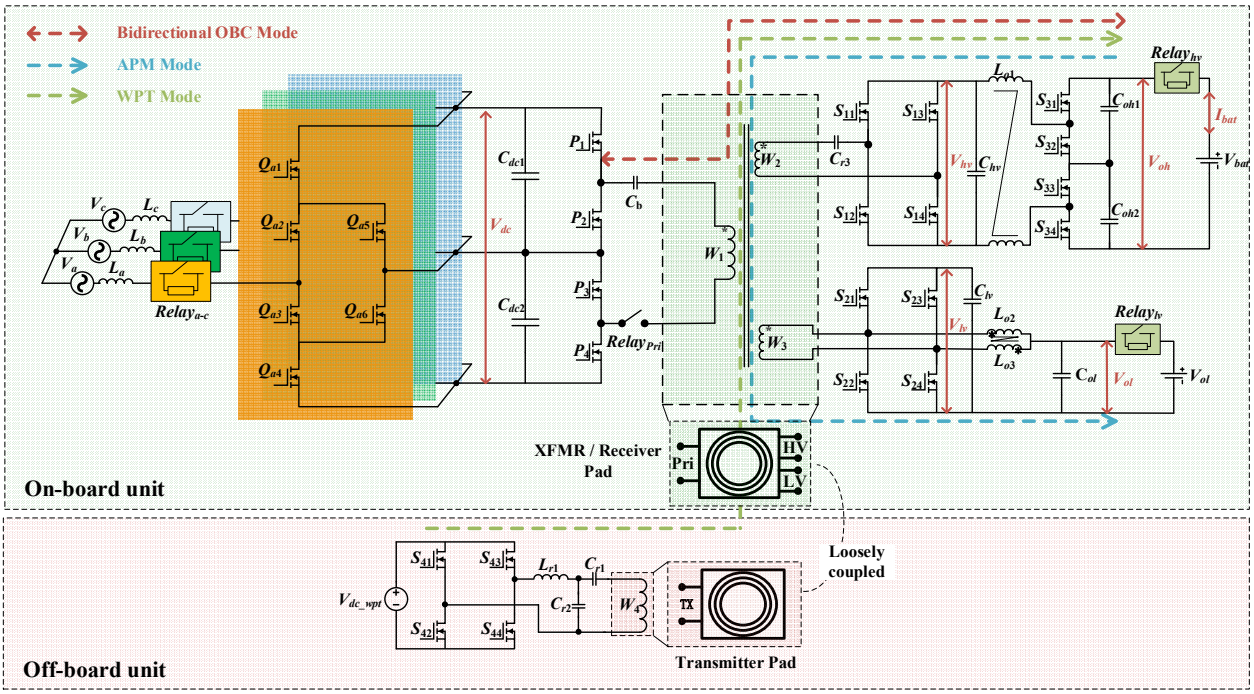

Fig. 1. proposed integrated multi-function and multi-level EV charger.

receiving (Rx) coil was added to a traditional OBC system to share the HV secondary side. The magnetic coupler integration is achieved in [7].

Inspired by the above, a highly integrated solution that provides WPT, OBC, V2L and APM is proposed in this paper, as illustrated in Fig. 1. The on-board unit of the proposed charger employs several stages and GaN devices are utilized to achieve compact design and high efficiency. Before connecting to the active AC grid and batteries, the DC bus capacitors, e.g. C_{dc} and C_{hv}, are fully discharged, which can yield large inrush current when plugged in. On the other hand, the starting process of different stages also needs to be regulated based on different functions. The dc-dc stage employs dual-active-bridge (DAB) topology. In [8], [9], two-phase and three-phase (3P) start-up procedures are proposed separately. In [10], authors proposed a new simple start-up scheme based on extended phase-shift (EPS) modulation, which can accelerate the start-up process and overcome the DC bias in the initial several switching periods. The soft start-up procedures for a two-stage AC/DC converter is proposed in [11], [12], where the DC/DC stage achieves soft starting by regulating the DC-link voltage. The soft start-up and shut-down procedures for a WPT system is also benchmarked in [13].

The literatures mentioned above mainly focus on the soft start-up and shut-down procedure of a single-stage converter or converters with simple functions, however, the comprehensive system-level soft start-up and shut-down procedures for integrated EV chargers with multiple stages and functions are not explored yet. This paper proposed a comprehensive system-level start-up and shut-down schemes for OBC, WPT and V2L in the proposed integrated EV charger. The rest of this paper is arranged as follows. The system configuration, the operation principle and the potential risk without soft start-up and shutdown for OBC, V2L and WPT modes are introduced in Sec. II. Sec. III details the proposed soft start-up and shut-down schemes for different modes. In Sec. IV, the experimental results and analyses are provided. Conclusion is drawn in Sec. V.

II. System Configuration , Operation Principle and Problems Statement

As shown in **Error! Reference source not found.**, the system consists of on-board and off-board unit. The off-board unit consists of the inverter, transmitter-side compensation circuit and the transmitter pad for the WPT system. The on-board unit includes one integrated pad, one 3P AC/DC converter and one triple active bridge (TAB) DC/DC converter, coupled by a three-port integrated pad. Three coils are integrated in this pad, i.e., the primary winding W_1, the HV secondary winding W_2 and the LV secondary winding W_3, all coupled closely. One non-isolated DC/DC converter is connected to the HV secondary side. To achieve higher power density, 650V and 100V GaN devices are used in this system. In order to receive 480VAC and 400V/800V HV batteries, the rated operation voltage on DC-link capacitor and output capacitors, i.e., V_{dc} and V_{oh}, are set to 800V. Therefore, a three-level structure is used on the primary side and the non-isolated DC/DC converter. The proposed charger is controlled by dual-digital signal processors (DSP), using CAN communication to link DSPs with vehicle control module (VCU).

A. OBC mode

In OBC mode, the power flows from PFC, through DAB and boost converters to the HV battery. Under the steady state, triple

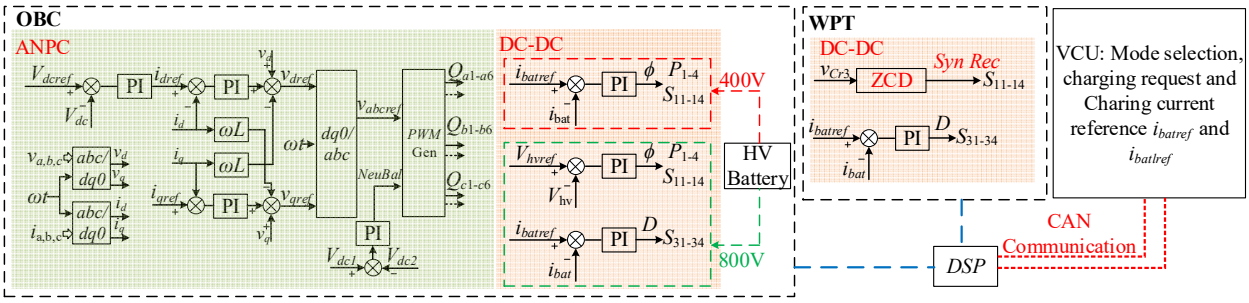

Fig. 2 Control diagram of different operation modes.

closed-loop proportional and integral (PI) controllers and SVPWM-based average current control are utilized at the PFC stage to regulate the DC-link voltage and power factor [14]. When charging a 400V battery, the DAB converter works under current close-loop control to modulate the charging power using the single-phase shift (SPS) modulation, and the boost will be bypassed by keeping S_{31} and S_{34} on, S_{32} and S_{33} off. When charging a 800V battery, the DAB converter works under SPS-based voltage closed-loop control to build a constant voltage on C_{hv}, and the output power is regulated by the boost converter by adjusting the duty cycle of four switches. The control diagram of the OBC mode is shown in Fig. 2. In this paper, only the case of charging 400V battery will be considered.

If directly enabling the closed-loop control of the PFC and DAB converters and bypass the boost converter with the active AC grid and battery plugged in, we can easily find that some inrush current due to instant voltage change of DC bus capacitors. Additionally, the unbalanced voltages at two sides of the DAB converter can cause the saturation of the PI controller and large inrush current in the transformer, which might cause the saturation of the magnetic core [10].

B. V2L mode

In V2L mode, the power flow is opposite to the OBC mode, i.e., power is transferred from HV batteries to the AC side. Only considering the 400V battery case, the boost is bypassed and DAB converter works under voltage closed-loop control. AC/DC converter works under voltage closed-loop control to regulate the output AC voltage. Without proper start-up procedure, the similar problems of OBC mode still exist.

C. WPT mode

In WPT mode, the power flows through the WPT and boost stage to the HV battery. The WPT stage consists of the WPT inverter, the LCC compensation network, the transmitter and receiver pads and the secondary rectifier with series (S) compensation. The resonant frequency, f_{WPT} is expressed as

$$2\pi f_{\mathrm{WPT}} = \frac{1}{\sqrt{L_2 C_{r3}}} = \frac{1}{\sqrt{L_{r1} C_{r2}}} = \frac{1}{\sqrt{\frac{L_4 (C_{r1} C_{r2})}{C_{r1} + C_{r2}}}} \tag{1}$$

Ignoring the coil resistance, the voltage gain is simplified as

$$G_v = \frac{M_{24}}{L_{r1}} \tag{2}$$

where M_{24} is the mutual inductance between W_2 and W_4.

Basically, the WPT stage will run under the open-loop control and generate a relatively stable output voltage on C_{hv}, and the boost stage will run under a current close-loop control to regulate the charging power. The implementation of the communication-less synchronized rectifier control (SRC) could help to increase the efficiency by reducing the loss on the secondary-side rectifier [15]. The principle is generating the synchronization signal by the zero voltage crossing point detection (ZVD) of the resonant capacitor, i.e., C_s. Because S compensation is utilized at the rectifier side, there is 90° phase difference between the voltage and current on C_s naturally. Therefore, the zero current crossing point detection (ZCD) of switches can be achieved. The control diagram of WPT mode is also shown in Fig. 2.

The main challenges for starting and shutting down the WPT system with the SRC control is that the SRC relies on the detection of ZVC point of C_s. However, at the very first several cycles, the voltage across C_s is not in the steady state and hard to predict, which might cause the wrong synchronization signals and large circulating current. Another concern is the start-up procedure of the following DC/DC converter. When charging the HV battery, it works as a boost converter. The voltage and current of inductor can be expressed as

$$L_{o1}\frac{di}{dt} = \begin{cases} V_{hv} - V_{oh} & ,when\ S_{31}\ and\ S_{34}\ is\ on \\ V_{hv} & ,when\ S_{33}\ and\ S_{33}\ is\ on \end{cases} \tag{3}$$

Based on (3), In one duty cycle， the current change can be expressed as

$$\Delta i = \frac{DT}{L_{o1}}(V_{hv} - V_{oh}) = \frac{(1-D)T}{L_{o1}}V_{hv} \tag{4}$$

where D is the duty cycle of S_{31} and S_{32} and T is the switching period. From (2), it is possible that the boost converter generates over current to the battery, which can trigger the over current protection or cause damage on the converter or the battery, if the initial battery voltage and initial voltage generated by the WPT stage are not considered.

III. Proposed Soft Start-up and Shut-down Schemes

Based on the analyses in Sec. II, the soft start-up and shut-down procedures should include two parts, i.e., pre-charging of

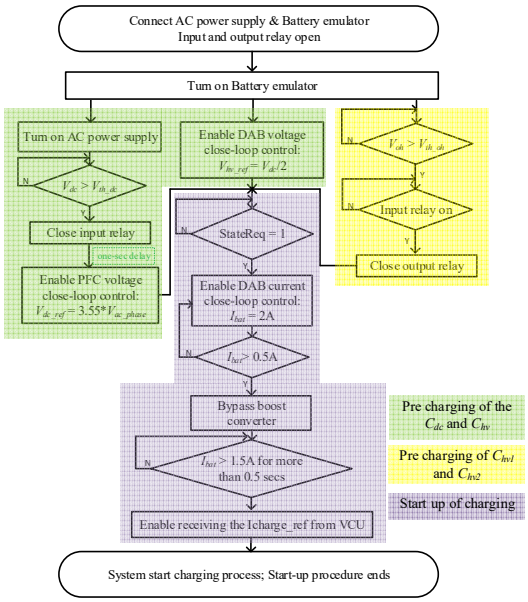

Fig. 3. Proposed start-up scheme for the OBC mode.

the large DC-link capacitors in the multi-stage system, and the appropriate converter-level soft start when active power sources are connected. Based on the different system configuration of each mode, details of proposed system-level start-up and shut-down schemes are introduced in this section. All schemes will be introduced following the same structure, which is the stand-by state of each stage, the right procedure of connection and disconnection of the active source, and the converter-level start-up strategy for each converter. In the lab test environment, we use a 3P AC source and an electric battery emulator to emulate the 3P AC grid and the HV battery pack on the EVs. The laptop emulates the VCU by running software CANalyzer on it.

A. OBC mode

The proposed soft start-up procedure is shown in Fig. 3. Initially, the input and output relay are open. PWMs of the PFC stage are disabled. DAB is running under the voltage closed-loop control and the reference is set to half of the DC-link voltage, V_{dc}. The boost converter is shut down too.

The start-up procedure is as follows.

Step 1: The HV battery is connected to the charger output, pre-charging the output capacitor, C_{hv1} and C_{hv2} through the paralleled resistor on the output relay, $Relay_{hv}$.

Step 2: The 3-Φ AC source is turned on, which emulates the charging gun is plugged in. C_{dc1}, C_{dc2} and C_{hv} are pre-charged by reverse conducting the PFC stage switch.

Step 3: V_{dc} is monitored by the controller, and the input relay will be closed after V_{dc} is reaches the threshold voltage, $V_{th\text{-}dc}$, which is set to 0.8 times of the root-mean-squared (RMS) value of phase AC voltage in the proposed hardware. The ratio of the $V_{th\text{-}dcbus}$ and the RMS value of phase AC voltage is determined by the pre-charging resistance.

Step 4: The output relay at HV battery side will be closed after the input relay, with a 0.5 seconds' delay.

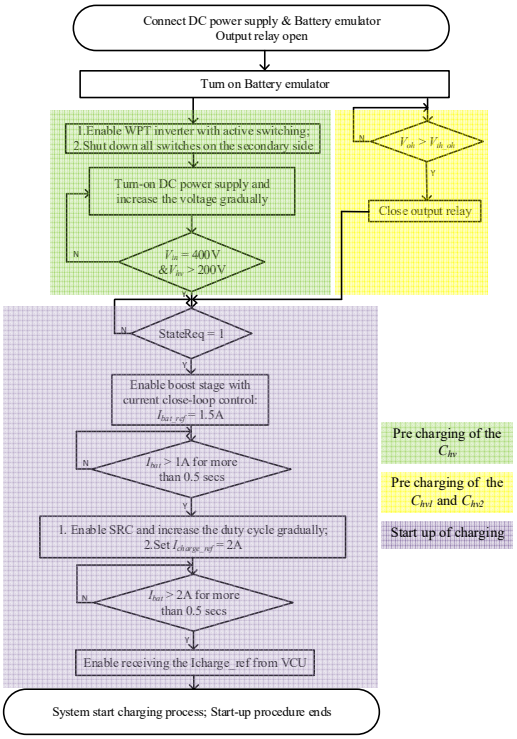

Fig. 4. Proposed start-up scheme for the WPT mode.

Step 5: PFC runs under voltage closed-loop control. The DC-link capacitors can be pre-charged further by increasing the DC bus voltage reference, $V_{dc\text{-}ref}$, to the rated value gradually. Since the DAB stage runs under voltage closed-loop control, C_{hv} is also pre-charged when C_{dc1} and C_{dc2} are pre-charged.

The first five steps finish pre-charging DC-link capacitors. Then, the charger will go to the "standby" state and DSPs will wait for the charging command from VCU.

Step 6: After receiving the charging command, the DAB runs under the current closed-loop control and the boost stage is still off. Therefore, the power flow can be limited to only from AC to HV battery, which can avoid the inrush current caused by much higher voltage on the battery. Gradually increasing duty cycle, we start to charge the battery with a small current.

Step 7: When battery current reaches the threshold, the boost converter is bypassed by switching S_{31} and S_{34} to reduce the conduction loss.

Step 8: After 0.5 seconds' delay, the charger starts charging the battery based on the battery current command from VCU.

When "Stop charging" command is sent to DSP, the charger will shut down, with the procedure shown as follows.

Step 9: Reducing the phase shift of the DAB stage to 0.05.

Step 10: Shutting down the boost stage, and DAB stage is switched to the voltage closed-loop control.

Step 11: Turning off the AC source.

Step 12: Turning off the battery load. The input relay and output relay will be opened.

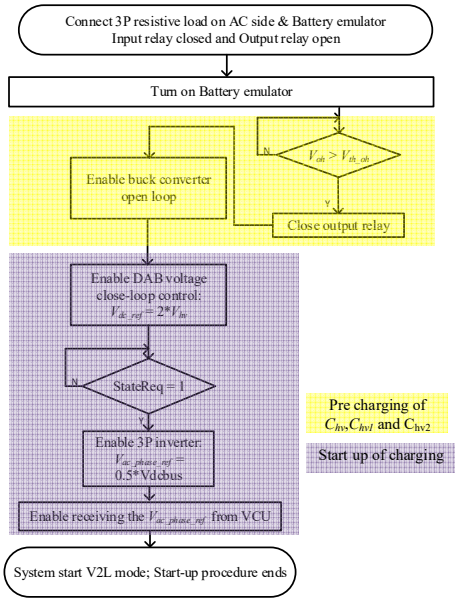

Fig. 5. Proposed start-up scheme for the V2L mode.

B. WPT mode

The proposed soft start-up procedure of the WPT mode is shown in Fig. 4. Initially, the output relay is open. The primary-side inverter runs under open-loop control with fixed frequency, f_{WPT} and 50% duty cycle. The secondary-side rectifier runs as a diode rectifier with all switches off. The boost converter is shut down as well.

The start-up procedure is as follows.

Step 1: The electric battery load is turned on which emulates the HV battery connected to the charger. Then, the output capacitors, C_{hv1} and C_{hv2}, will be pre-charged through the paralleled resistor on the output relay, $Relay_{hv}$.

Step 2: The inverter side DC power supply is turned on and increases the voltage to rated voltage gradually. At the same time, the DC-link capacitor, C_{hv}, will be pre-charged based on equation (2). The first two steps finish the pre-charging of the DC-link capacitor. Then, the charger will go to "Standby" and DSPs will wait for the charging command from VCU.

Step 3: After receiving the charging command, the boost stage runs under the current closed-loop control with the battery current reference of 1.5A, which can make sure the voltage across the C_{r3} large enough to be detected by the ZVC circuit correctly and reliably .

Step 4: After the battery current is greater than 1A, and this stage lasts more than 0.5 seconds, SRC will be enabled.

Step 5: System starts charging the battery and receiving the battery current reference from VCU. The output power is regulated by the boost stage.

When "Stop charging" command is sent to DSP, the charger will shut down as the procedure introduced as follows.

Step 6: Reducing the battery current reference to 1A.

Step 7: SRC of the secondary-side rectifier is disabled after the battery current drops below 1A.

Step 8: Reducing the battery current reference to 0, and then shut down the boost stage.

Step 9: The DC power supply at the inverter side is shut down.

Step 10: The battery load is shut down and the output relay will be opened.

C. V2L mode.

The proposed start-up procedure is shown in Fig. 5. For the V2L mode, only the resistive load is considered in this paper. Therefore, only one active source needs to be considered. Initially, the relay at the battery side is open and the relay on AC side is closed. The 3-Φ inverter is shut down, and the buck converter is bypassed by turning on S_{31} and S_{34}. The DAB stage runs under the voltage closed-loop control.

The start-up procedure is as follows.

Step 1: The electric battery load is turned on which emulates the HV battery connected to the charger. Then, the battery-side capacitors, C_{hv1} and C_{hv2}, will be pre-charged through the paralleled resistor of the output relay, $Relay_{hv}$.

Step 2: The $Relay_{hv}$ is closed after v_{oh} reaches the threshold value, v_{th_oh}. The pre-charging of C_{hv1} and C_{hv2} is finished.

Step 3: The buck converter runs open-loop control with the duty cycle of S_{31} increasing from 0.05 to 1. The DC-link capacitors C_{hv} is pre-charged.

The first 3 steps finish pre-charging DC-link capacitors. Then, the charger will go to standby, and DSPs will wait for the charging command from VCU.

Step 4: DAB voltage closed-loop control and inverter voltage closed-loop control will be enabled.

Step 5: System starts supplying power to the 3-Φ resistive load and receiving the AC voltage reference from VCU. The output power is regulated by the inverter.

Since there is only one active source in V2L mode, when "Stop charging" command is sent to DSP from VCU, the charger will shut down as follows.

Step 6: The DAB stage stops the closed-loop control, and the phase shift reduces gradually.

Step 7: When the current is less than 1A, the DAB stage and buck stage will be shut down at the same time.

Step 8: The battery emulator is shut down and the output relay is opened.

IV. Experimental Results

As shown in Fig. 6, a prototype is built. The steady state of all operation modes is tested to verify the OBC, WPT and V2L functions of the prototype. Then, the proposed soft start-up and shut-down procedures for different modes are verified on this prototype.

(a)

(b)

Fig. 6. Experimental prototype: (a) On-board unit, (b) Off-board unit.

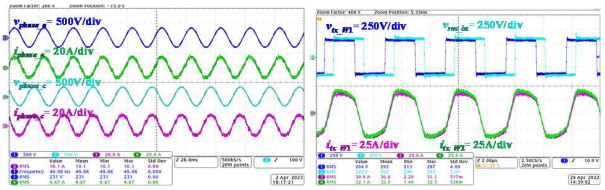

(a) (b)

Fig. 7. OBC test waveform. (a) PFC stage, (b) DAB stage.

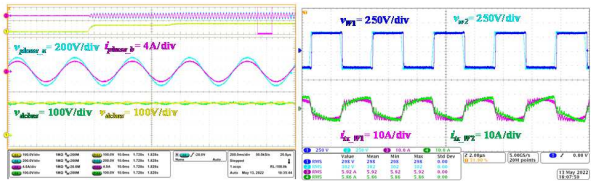

(a) (b)

Fig. 8. V2L test waveform. (a) Inverter stage, (b) DAB stage.

A. *Steady state operation*

Fig. 7 illustrates the steady-state waveform of the PFC stage and DAB stage at the OBC mode. Fig. 8 illustrates the steady-state waveform of PFC stage and DAB stage at V2L mode. Fig. 9 illustrates the steady-state waveform of the inverter stage and rectifier stage at WPT mode. Experimental results verified the proposed integrated charger can achieve all the functions.

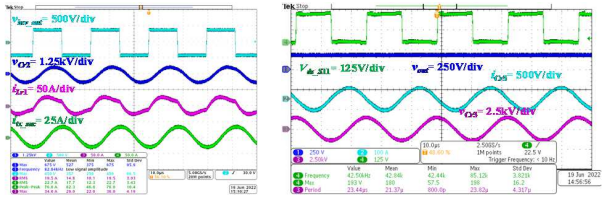

(a) (b)

Fig. 9. WPT test waveform: (a) inverter stage, (b) Rectifier stage.

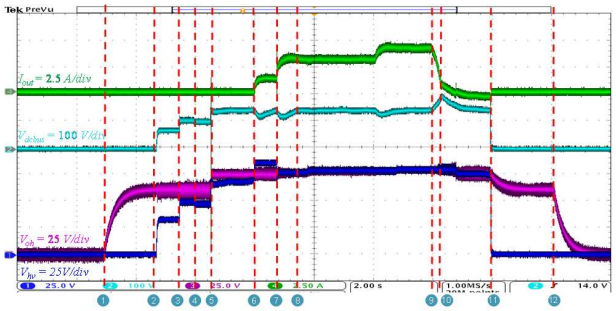

(a)

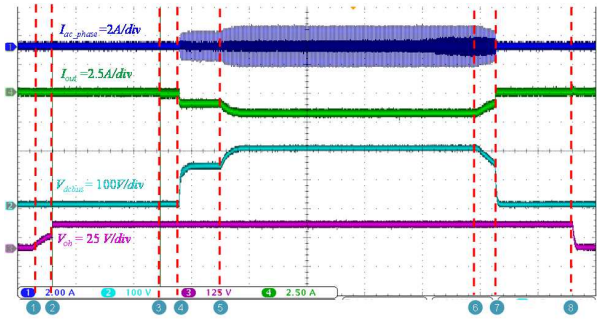

(b)

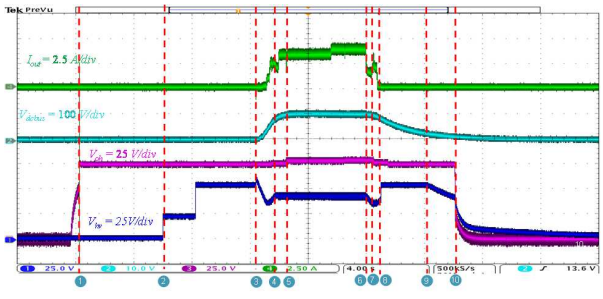

(c)

Fig. 10. Complete charging procedures with proposed soft start-up and shut-down schemes. (a) OBC mode with $60VAC_{phase}/75V_{bat}$, (b) V2L mode with $100V_{bat}$, (c) WPT mode with $100VDC_{in}/75V_{bat}$.

B. *Soft start-up and shut-down procedures*

The down-scale complete charging procedures are shown in Fig. 10. The battery current, the DC-link voltages, i.e., V_{dc}, V_{oh}, V_{hv}, are recorded in all modes, from where we can find that no large inrush current in or out the battery. Besides, all the DC-link voltages change softly without serious overvoltage, which is benefited from the proposed proper pre-charging strategies in schemes.

As shown in Fig. 10, the effectiveness of the proposed soft start-up and shut-down schemes for OBC, V2L and WPT modes is verified, which means the charger can be connected to the active 3P AC source, the HV battery directly and 3P resistive load. This is aligned with the practical scenarios that 1) the EV users plug the charger gun into the EV; 2) park at the wireless charging station when they would like to charge their EVs, and 3) Supply power to any resistive load using the HV batteries on their EV. The capability of starting, shutting down the system and changing the power remotely by the VCU through CAN communication, which is essential function of the EV charger in real-world EV charging, is also verified.

V. Conclusions and Future Work

This paper introduces a highly integrated EV charger. Based on the real-world EV charger application, the practical ,comprehensive and reliable system-level start-up and shut-down schemes for the OBC, WPT and V2L modes of the charger are proposed. With the proposed schemes, the system can achieve soft start-up without large inrush current, and the system can be controlled to start, shut down or change power by VCU remotely through CAN communication. The prototype and the effectiveness of the proposed schemes have been thoroughly verified by experiments. Future work will include converter-level soft start-up strategies based on the different control strategies of each stage for different applications.

References

[1] H. K. Bai *et al.*, "Charging Electric Vehicle Batteries: Wired and Wireless Power Transfer: Exploring EV charging technologies," *IEEE Power Electron. Mag.*, vol. 9, no. 2, pp. 14–29, Jun. 2022.

[2] G. Yu and S. Choi, "An Effective Integration of APM and OBC With Simultaneous Operation and Entire ZVS Range for Electric Vehicle," *IEEE Trans. Power Electron.*, vol. 36, no. 9, pp. 10343–10354, Sep. 2021.

[3] I. Kougioulis, P. Wheeler, and M. R. Ahmed, "An Integrated On-Board Charger and Auxiliary Power Module for Electric Vehicles," in *2022 IEEE Applied Power Electronics Conference and Exposition (APEC)*, Mar. 2022, pp. 1162–1169.

[4] L. Zhu, H. Bai, A. Brown, and L. Keuck, "A Current-fed Three-port DC/DC Converter for Integration of On-board Charger and Auxiliary Power Module in Electric Vehicles," in *2021 IEEE Applied Power Electronics Conference and Exposition (APEC)*, Jun. 2021, pp. 577–582.

[5] Y. Zhang *et al.*, "Misalignment-Tolerant Dual-Transmitter Electric Vehicle Wireless Charging System With Reconfigurable Topologies," *IEEE Trans. Power Electron.*, vol. 37, no. 8, pp. 8816–8819, Aug. 2022.

[6] M. Elshaer, C. Bell, A. Hamid, and J. Wang, "DC–DC Topology for Interfacing a Wireless Power Transfer System to an On-Board Conductive Charger for Plug-In Electric Vehicles," *IEEE Trans. Ind. Appl.*, vol. 57, no. 6, pp. 5552–5561, Nov. 2021.

[7] Y. Zhang *et al.*, "Integration of Onboard Charger and Wireless Charging System For Electric Vehicles With Shared Coupler, Compensation, and Rectifier," *IEEE Trans. Ind. Electron.*, vol. 70, no. 7, pp. 7511–7514, Jul. 2023.

[8] C. Gammeter, F. Krismer, and J. W. Kolar, "Comprehensive Conceptualization, Design, and Experimental Verification of a Weight-Optimized All-SiC 2 kV/700 V DAB for an Airborne Wind Turbine," *IEEE J. Emerg. Sel. Top. Power Electron.*, vol. 4, no. 2, pp. 638–656, Jun. 2016.

[9] P. Yao, X. Jiang, and F. F. Wang, "Soft Starting Strategy of Cascaded Dual Active Bridge Converter for High Power Isolated DC-DC Conversion," in *2020 IEEE Applied Power Electronics Conference and Exposition (APEC)*, Mar. 2020, pp. 1031–1037.

[10] X. Liu *et al.*, "A Simple and Fast Start-up Strategy for Dual Active Bridge Converters with DC Bias Suppression," *IEEE Trans. Power Electron.*, pp. 1–10, 2023.

[11] L. Cheng *et al.*, "An Optimized Start-up Method for Modular Cascaded AC/DC Power Electronic Transformer with Minimized Input-Inrush Current in Dual Active Bridge," in *2020 IEEE 9th International Power Electronics and Motion Control Conference (IPEMC2020-ECCE Asia)*, Nov. 2020, pp. 2402–2407.

[12] G. Jean-Pierre, A. K. Tripathi, V. Burugula, and V. Bhavaraju, "An Optimized Start-up Scheme for Isolated Cascaded AC/DC Power Converters," in *2022 IEEE Energy Conversion Congress and Exposition (ECCE)*, Oct. 2022, pp. 1–6.

[13] C. Riekerk, F. Grazian, T. B. Soeiro, J. Dong, and P. Bauer, "Study on Soft Start-Up and Shut-Down Methods for Wireless Power Transfer Systems for the Charging of Electric Vehicles," in *2021 IEEE PELS Workshop on Emerging Technologies: Wireless Power Transfer (WoW)*, Jun. 2021, pp. 1–6.

[14] X. Guo, H.-P. Ren, and D. Liu, "An Optimized PI Controller Design for Three Phase PFC Converters Based on Multi-Objective Chaotic Particle Swarm Optimization," *J. Power Electron.*, vol. 16, no. 2, pp. 610–620, 2016.

[15] S. Cochran and D. Costinett, "Discrete Time Synchronization Modeling for Active Rectifiers in Wireless Power Transfer Systems," in *2019 20th Workshop on Control and Modeling for Power Electronics (COMPEL)*, Jun. 2019, pp. 1–8.